

Time-Resolved Electronic Spectroscopy of 2,2'-Bisindene

A Senior Honors Thesis

Presented in Partial Fulfillment of the Requirements for graduation *with research distinction* in  
Chemistry in the undergraduate colleges of The Ohio State University

by

Adam David Dunkelberger

The Ohio State University

June 2007

Project Advisor: Terry L. Gustafson

## Abstract

The model polyene, diphenylbutadiene (DPB), exhibits two closely-spaced first and second electronic excited states. The excited state lifetime of DPB varies significantly with solvent. To probe these excited states, ultrafast laser spectroscopy techniques, such as femtosecond transient absorption, must be used. Our goal is to better understand how structure and solvent effects affect the excited states. The understanding we gain can then be further applied to more complex, highly chiral molecules that may have interesting opto-electronic applications. At the present time, my research focuses on synthesizing rotationally constrained DPB analogues. There are three axes about which DPB can undergo intramolecular rotation, two of which are equivalent. Two molecules have been targeted for synthesis and analysis: 2,2'-bisindene, in which rotation about the two phenyl bonds is restricted, and [(3E)-3-benzylidenecyclopent-1-en-1-yl] benzene, in which rotation about the central single bond of the butadiene chain is restricted. My work has focused on 2,2'-bisindene. The synthesis of 2,2'-bisindene appears once in literature and is obtained through a Grignard self-coupling of 2-bromoindene. The synthesis of 2,2'-bisindene proved much more difficult than expected. The precursor, 2-bromoindene, is obtained by acid catalyzed dehydration of 2-bromoindanol. Successful isolation of the 2-bromoindene required an adaptation of several techniques used in the literature. Through further adaptation of literature methods, I was able to synthesize pure 2,2'-bisindene in sufficient quantity and purity for spectroscopic analysis. I have obtained various steady-state and time-resolved electronic spectra of 2,2'-bisindene and compared them to literature results for DPB.

This thesis is dedicated to the memory of Charles Burns and Violet Dunkelberger, who are truly missed

## **Acknowledgments**

*Prof. Terry Gustafson*

My mentor, without whom this thesis would not be possible

*Prof. T.V. RajanBabu*

An excellent advisor and teacher who guided the synthetic phase of this project

*The Gustafson, Kohler, and RajanBabu Research groups*

for providing help and encouragement throughout the project

*Mrs. Maria Elliott*

for fostering my love of chemistry

*My Parents and Siblings*

for enduring countless lectures on spectroscopy and quantum mechanics

*The Camille and Henry Dreyfus Foundation*

for graciously funding my research during the summer of 2006 through the Jean Dreyfus-Boissevain Undergraduate Scholarship for Excellence in Chemistry

*The Colleges of the Arts and Sciences Honors Research Scholarship*

for providing funding for my research from 2005-2007

## Table of Contents

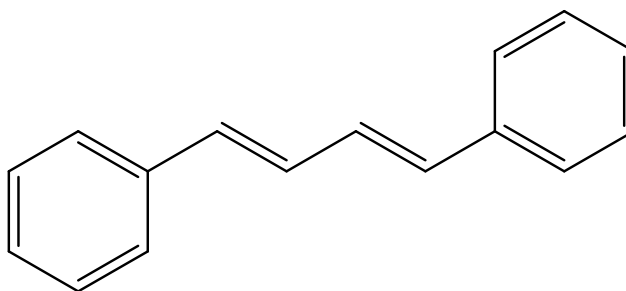
Abstract	i
Acknowledgments	ii
Table of Contents	iii
1. Introduction	1
1.1. 2,2'-Bisindene as a Model Compound	1
1.2. Absorption and Emission Processes of Interest	2
1.3. Time-Correlated Single Photon Counting	3
1.4. Anisotropy	13
1.5. Transient Absorption	15
1.6. Synthetic Considerations	16
2. Results and Discussion	18
2.1. Synthesis of 2,2'-Bisindene	18
2.2. Absorption and Fluorescence Spectra	20
2.3. TCSPC Lifetime and Anisotropy	21
2.4. Pump-Probe Lifetime and Anisotropy	23
2.5. Broadband Transient Absorption	25
3. Conclusions and Future Considerations	28
Appendix – NMR Spectra of Synthesized Compounds	29
References	35

## 1. Introduction

### 1.1. 2,2'-Bisindene as a Model Compound

In 1956, Brown and Wald reported the 11-*cis* structure of retinal and the photoisomerization of the compound.<sup>1</sup> This breakthrough gave unprecedented insight into the molecular basis of vision. In 1967, Wald was awarded the Nobel Prize in Medicine in recognition of “discoveries concerning the primary physiological and chemical processes in the eye.”<sup>2</sup>

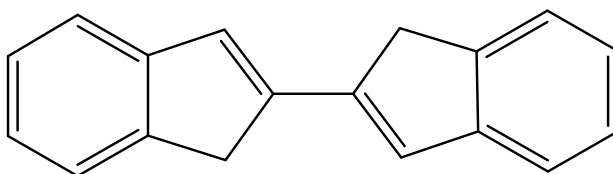
The *cis-trans* isomerization of retinal can be viewed as one of the first ultrafast phenomena observed by researchers. Ultrafast spectroscopists continue to work to understand the excited state dynamics of conjugated poly-ene systems which act as models for retinal. One such model compound is 1,4-diphenylbutadiene (DPB).



1,4-diphenylbutadiene

DPB possesses two closely ordered, short lived excited electronic states whose ordering is dependent on solvent. It has been hypothesized that the two excited states arise from *s-cis-s-trans* isomerization; one state is thought to arise from the more stable *s-trans* conformer, while the other is thought to arise from the *s-cis*. Extensive work has been performed with DPB analogues in which rotation about the central single bond is restrained.

This thesis describes the synthesis and analysis of a DPB analogue in which rotation about the phenyl bonds is constricted, 2,2'-bisindene. Through steady state and time resolved electronic spectroscopy, the effect of phenyl rotation on the photophysics of DPB is explored.



2,2'-bisindene

## 1.2. Absorption and Emission Processes of Interest

Quantum mechanics dictates that the electronic, vibrational, and rotational states of atoms and molecules exist as quantized energy levels. The populations of these states are dependent upon the energy of the system. The spacing of the energy levels can be probed through spectroscopic techniques. The electronic energy levels of 2,2'-bisindene are explored in this thesis through use of absorption, fluorescence, and transient absorption spectroscopy. All of these processes are probed with light in the ultraviolet-visible range, with wavelengths between 200 and 800 nm.

Electronic absorption occurs when light incident upon a molecule triggers an excitation from one electronic state to another. The ground state, the populated state of the highest energy, is generally a singlet state – a state in which the spins of the electrons “cancel” each other. This singlet ground state is called the  $S_0$  state. Absorption spectroscopy, also known as UV/Vis spectroscopy, probes transitions from the  $S_0$  state to excited states  $S_n$ .

Electronic excitations can access different vibrational levels of the excited state. In gas-phase electronic spectra, the vibrational structure of the analyte is readily apparent. The vibrational bands of analytes in solution are significantly blurred by interactions between the usually dilute solute and solvent, resulting in very broad absorption bands.

After an electron is promoted to an excited state, it can decay through a multitude of radiative and non-radiative processes. One such radiative process is fluorescence, in which the electron decays from the ground vibrational state of the  $S_1$  state to the  $S_0$  state. This process results in the emission of a photon with wavelength characteristic of the energy gap between electronic states. The excited molecule exists for a finite time period which can be measured through time-resolved spectroscopic methods.

While traditional UV/vis spectroscopy measures the absorption of the  $S_0$  state, transient absorption techniques measure the absorption of the  $S_1$  state, the “transient” species. Because of the very short lifetimes of the transient state, transient absorption measurements require very short pulses of light and incredible control of the pulse delays. Ultrafast spectroscopy methods have made transient absorption increasingly practical.

### **1.3. Time-Correlated Single Photon Counting**

When studying photochemical reactions such as photoisomerization, it is important to obtain accurate fluorescence lifetime measurements. Time-correlated single-photon counting (TCSPC) is an effective way of gathering such data.

Before the advent of TCSPC in 1961, fluorescence lifetimes were measured using either modulation or pulse-sampling methods.<sup>4</sup> These methods were often insensitive and it was difficult to measure lifetimes shorter than about 7 ns.<sup>4</sup> TCSPC allows for much greater sensitivity and for the accurate determination of much shorter lifetimes.

A TCSPC measurement is made by exciting a sample, collecting an emitted photon from the sample, and measuring the time between the excitation and emission. Figure 1.3.1, adopted from Lakowicz,<sup>5</sup> illustrates a basic schematic of a TCSPC experimental setup.

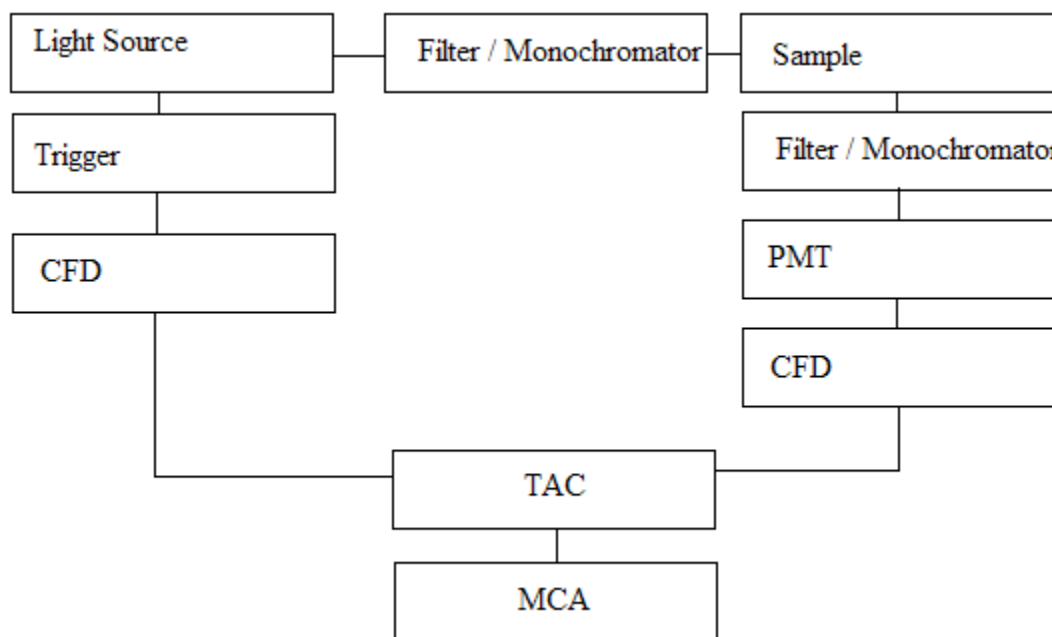


**Figure 1.3.1. Schematic Diagram of Generic TCSPC Setup**

In a generic TCSPC experiment, the source emits a short pulse of radiation which triggers a time-to-amplitude converter (TAC) to “start” while exciting the sample. When the sample emits, the resulting photon causes the TAC to “stop.” Between the start and stop pulses, a voltage builds in the TAC. As stated by Lakowicz, “A multichannel analyzer (MCA) converts this voltage to a time channel [... and] builds up a probability histogram of counts versus time channel.<sup>5</sup>” It is this histogram which is analyzed to calculate the fluorescence lifetime of the sample.

Various light sources can be used for TCSPC experiments. Lasers are obvious choices, since the method requires short, intense pulses of incident radiation. Picosecond dye lasers are



often used. They can offer pulses as narrow as 5 ps and a variety of dyes are available to produce radiation of a wide range of wavelengths.<sup>5</sup> Titanium:sapphire lasers and solid state lasers offer shorter pulses, but are newer and more expensive than dye lasers.<sup>5</sup> A picosecond dye laser was used for the collection of TCSPC data in this thesis.

Before wide availability of lasers, flashlamps were used to excite samples for TCSPC experiments. Flashlamps “...typically provide excitation pulses about 2 ns wide, with much less power than is available from a laser source.”<sup>5</sup> These wide pulses exacerbate the problem of convolution in analyzing TCSPC data.

A variety of specialized electronic equipment is needed for TCSPC experimentation. Constant fraction discriminators help to provide “the highest possible time resolution” by minimizing the effects of the non-uniform distribution of pulse heights from the source.<sup>5</sup> Along with the aforementioned TAC and MCA, amplifiers and delay lines are used to further facilitate the collection of data.<sup>5</sup>

Lakowicz posits that the detector is, “Perhaps the most critical component for timing.”<sup>2</sup> Photomultiplier tubes (PMTs), whether microchannel plate (MCP) or dynode chain, are the detectors of choice for TCSPC experiments. Dynode chain PMTs are capable of time resolutions as low as 112 ps, while MCP PMTs have recorded pulses as short as 25 ps.<sup>5</sup> Photodiodes are typically not used for TCSPC experiments due to issues with gain and small active areas.<sup>5</sup>

The underlying physical principle that makes TCSPC a useful technique is, “...the concept that the probability distribution for emission of a single photon after an excitation event yields the actual intensity against time distribution of all the photons emitted as a result of the

excitation.<sup>4</sup>” It is for this reason that the histogram obtained can be directly correlated to the actual emission lifetime.

Three major issues arise in the collection and interpretation of TCSPC data. The first is “pulse pileup.”<sup>5</sup> Because the first photons to arrive at the TAC stop the measurement, the observed fluorescence lifetime will be shorter than the actual value if pulse pileup is not accounted for. The most common method used to correct for pulse pileup is reducing the rate at which photons are counted. Collecting only one photon per 100 excitation pulses generally gives accurate lifetimes.<sup>5</sup> The drawback of this method is the long collection time needed to gather accurate data. The TCSPC system used in this thesis employs an iris to limit the number of photons incident upon the detector. Data collection times fell between 1 h and 3 h.

The second issue is the nature of the excitation pulse. If the excitation pulse were infinitely narrow (a  $\delta$  function), the data collected would represent the true time-resolved intensity, but all sources emit radiation in pulses with non-zero widths and varying amplitudes.<sup>5</sup> With a common dye laser, the lamp profile in Figure 1.3.2 was obtained.

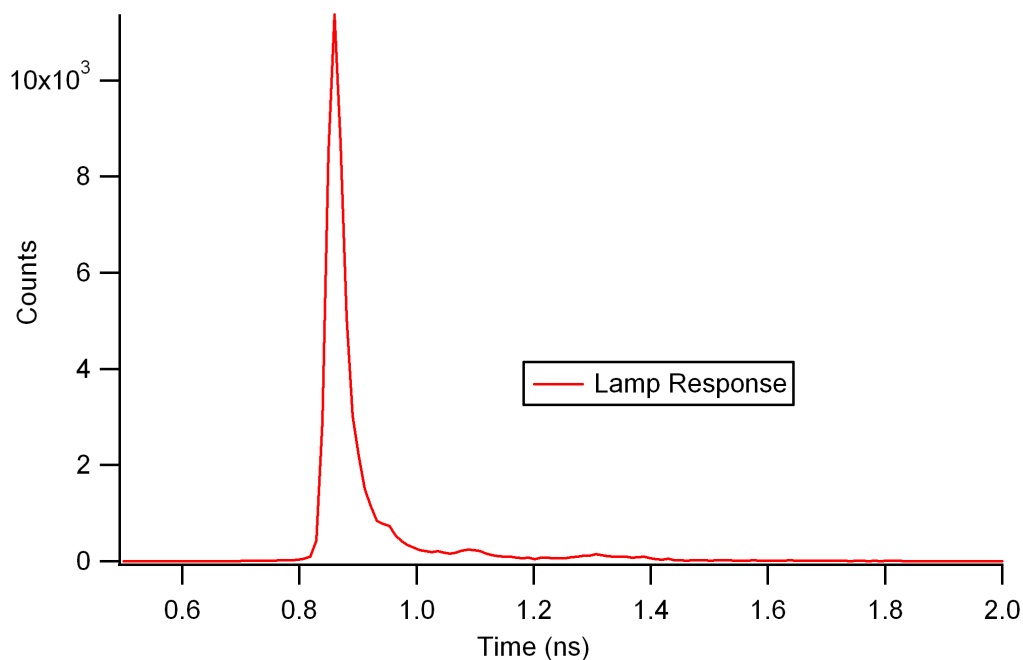


**Figure 1.3.2. Typical Lamp Profile of Dye Laser**

To obtain an accurate lifetime, one must convolute the observed fluorescence lifetime data with the lamp function. This task is performed by breaking the lamp function into  $\delta$  functions and treating the decay as a sum of the responses caused by each of the  $\delta$  functions.<sup>5</sup> Practically, this convolution is performed with data analysis programs. One such program, written by the Gustafson group, was used to process the data collected in this thesis.

The third issue to be dealt with is conversion from channels to time. The MCA provides a histogram of collected photons in bins corresponding to channels. Each channel corresponds to a segment of time. The instrument can be calibrated by using a second pulse from the source after a predetermined delay to stop the VAC rather than emission from a sample. By counting the channels between the two pulses, one can calculate the amount of time that each channel corresponds to. Figure 1.3.3 shows the data from a calibration with an 8 ns pulse delay.

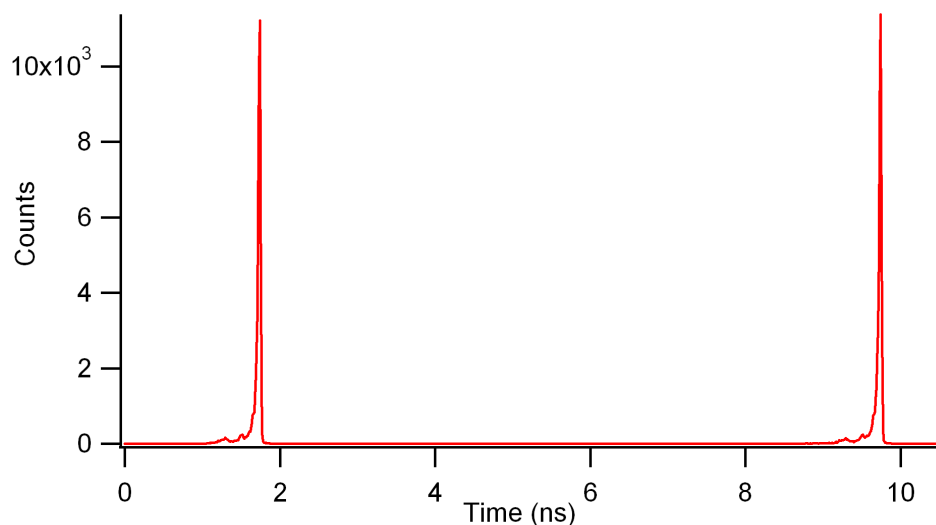


**Figure 1.3.3. Typical Delay Calibration Data, Calibration Already Performed**

The primary benefit of TCSPC is the variability of the instrumental setup. A wide range of components can be used to perform TCSPC experiments. Commonly available components such as dye lasers and dynode chain PMTs are capable of accurate measurement, albeit with less resolution than their more expensive counterparts. There are two useful alternatives to TCSPC: streak cameras and fluorescence upconversion.

Streak cameras represent a progression of technology from the previously mentioned pulse-scanning methods.<sup>4</sup> These instruments allow for simultaneous measurement of wavelength and time-resolved decays and offer faster response functions than TCSPC.<sup>5</sup> Streak cameras, however, have difficulty with complex decays due to a small intensity range and low signal-to-noise ratio.<sup>5</sup>

Fluorescence upconversion methods offer much better time resolution than TCSPC but are prohibitively complex. Lakowicz states that, "...even a seemingly minor change of the

emission wavelength can require a major readjustment of the apparatus...<sup>5</sup>” It is also difficult to measure long (>1-2 ns) decay times with upconversion instruments.<sup>5</sup>

TCSPC allows for the determination of multiexponential decay functions. This capability is of utmost importance to the study of photoisomerization. Multiexponential decays show that more than one decay process is available to the excited state. If a molecule is excited and isomerizes, the newly formed isomer will generally have a different lifetime from that of the original isomer. This capability is of great use in exploring the phenomenon of DPB photoisomerization.

Lifetimes measured with TCSPC offer no insight as to the structure of the compounds analyzed. Other time-resolved spectroscopic methods, such as transient absorption or time-resolved vibrational spectroscopy, must be used to determine the structure of the compounds of interest.

Four recent journal articles show the breadth of use of TCSPC in the study of photoisomerization reactions. Canonica *et al.* used TCSPC in a study of fluorescent whitening agents (FWAs).<sup>6</sup> These compounds are “largely used in textile and paper manufacturing and in household detergents.”<sup>6</sup> Because of their use as detergents, FWAs are common pollutants, but they are not biodegradable. They are, however, photodegradable – the E isomers are more susceptible to photodegradation due to their higher extinction coefficients at relevant wavelengths. When excited, these compounds can switch from the E to Z configuration. Figure 1.3.4 shows the compounds studied by Canonica, *et al.*

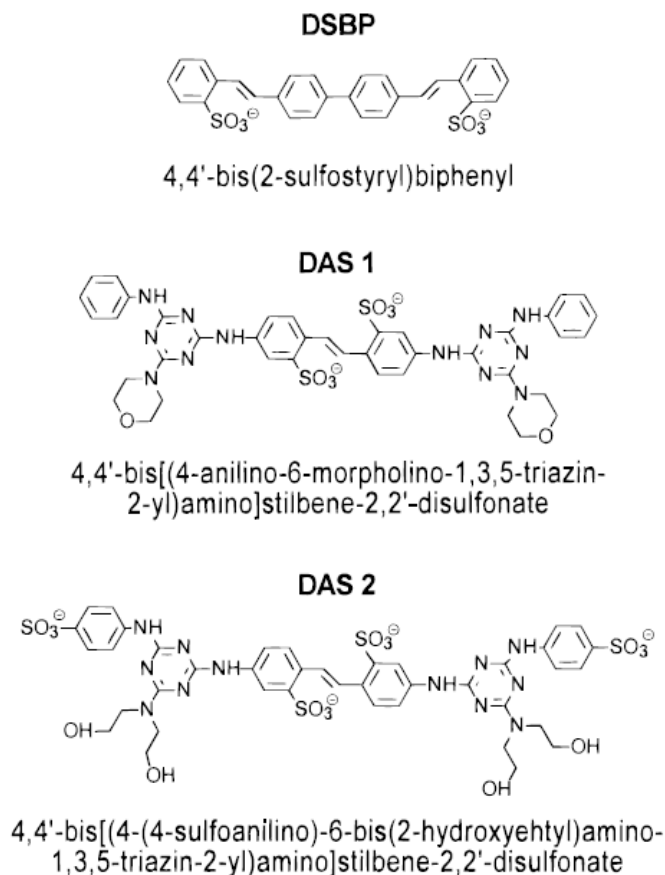


**Figure 1.3.4. Structures and Names of the FWAs<sup>6</sup>**

Canonica *et al.* used a mode-locked Nd:YAG laser and sulforhodamine B dye laser as the excitation source and a MCP-PMT as the detector. According to the paper, “With this setup, one can achieve apparatus response functions as short as 80 ps fwhm [full width half max].<sup>6</sup>” The TCSPC system was used to probe the kinetics of the photoisomerization equilibrium and determine the % E-isomer, a useful measure of the propensity to photodegrade.

Petrov, *et al.*<sup>7</sup> used TCSPC to investigate the effects of solvation on the photoisomerization of a cyanine dye, DTCl (see Figure 1.3.5). Table 1.3.1 shows the results of the fluorescence lifetime measurements performed by Petrov, *et al.* They suggest that the longer lifetime is due to photoisomerization to a cis form. They conclude that, “...preferential solvation

of thiocarboanion dies in binary mixtures ... leads to a significant diminution of isomerization efficiency...<sup>7</sup>”

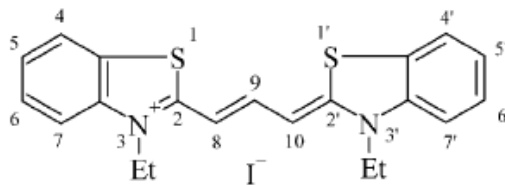


**Figure 1.3.5. Structure of DTCl<sup>7</sup>**

**Table 1.3.1 Fluorescence Lifetimes  $\tau_i$  for Various Volume Fractions of DMSO in Mixtures with Toluene (Excitation Wavelength 570 nm; Emission Recorded at 585 nm)<sup>7</sup>**

DMSO, vol %	$\tau_1$ , ps	$\tau_2$ , ps
100	299	
20	295	
17	335	
14	284	452
12	236	419
8	178	497
6	507	
3.2	629	
1.6	684	

Seixas de Melo *et al.*<sup>8</sup> used TCSPC to explore the kinetics of an intramolecular photon transfer reaction in indigo and its derivatives. Intramolecular proton transfer is an example of constitutional photoisomerization. A homemade TCSPC system with a resolution of 150 ps was used to measure the lifetimes of the keto and enol forms of the compounds of interest. This data was then used to calculate the rate constant of the excited state proton transfer (ESPT) reaction. Figure 1.3.6 shows a scheme from the paper in which the ESPT equilibrium of preCiba, an indigo derivative, is shown.

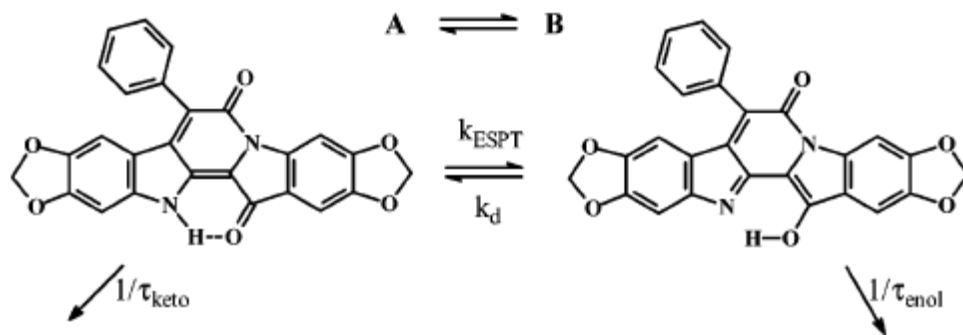


**Figure 1.3.6. ESPT Equilibrium Scheme<sup>8</sup>**

Another class of photoisomerization reactions is photocyclization. Karatsu, *et al.*<sup>9</sup> used TCSPC methods to probe the kinetics and reaction mechanisms of the cyclization of 1-(2-anthryl)-2-phenylethene (2APE) and its model compounds. Along with photocyclization, these compounds readily undergo photoisomerization about their double bonds, switching between E and Z configurations. Karatsu, *et al.* used a titanium:sapphire laser with a 150 fs pulse width pumped by an argon ion laser to perform TCSPC measurements.

Time-correlated single-photon counting offers accurate collection of fluorescence lifetime data which can be applied to the study of photoisomerization reactions. TCSPC is especially useful to the study of the kinetics of such reactions, but must usually be supplemented by other time-resolved spectroscopic methods to elucidate the structure of the participants in the excited state reactions.



## 1.4. Anisotropy

Molecules absorb and emit only light whose polarization matches the orientation of the molecule's electric dipole. This behavior can be exploited to study the motion of molecules in solution.

Ordinary spectroscopy is performed with unpolarized light. This unpolarized light interacts well with the random distribution of dipole orientations of the analyte. Anisotropy measurements are performed with polarizers which convert unpolarized light into plane polarized light of a specified angle. Anisotropy experiments involve the collection of two data sets: one in which the collected light is “parallel” to the incident light, and one in which the collected light is “perpendicular” to the incident light. In the course of this project, anisotropy data was collected with fluorescence through TCSPC and with transient absorption through single-wavelength pump-probe spectroscopy.

In a fluorescence anisotropy measurement, a polarizer gives the incident light a known angle, calibrated to be vertical with respect to the sample. This light then excites only molecules whose electric dipole is aligned with the light. The molecule then tumbles through solution until it decays, emitting light with a polarization equal to the new orientation of its dipole. A polarizer mounted between the sample cell and detector allows only light of a specified polarization to reach the detector.

For the “parallel” fluorescence trace, the second polarizer is set to the same angle as the first. The light collected is emitted from molecules whose orientation has changed very little over the lifetime of the excited state. In the “perpendicular” trace, the second polarizer is shifted to an angle perpendicular to the first.

The perpendicular trace is often rounded and much less intense than the parallel trace. This effect arises from the fact that all of the excited molecules begin in the perpendicular orientation. Some decay immediately, giving the sharp features of the parallel trace. Perpendicular light is not detected until the molecules have had time to reorient in solution and then emit.

In a pump-probe transient absorption anisotropy experiment, both the pump and probe pulses are polarized before reaching the sample. For the parallel trace, the pump and probe polarizers are set to the same angle. For the perpendicular trace, the polarization of the probe is changed. The parallel and perpendicular traces obtained through transient absorption techniques are very similar to those observed with fluorescence techniques. In the case of transient absorption, the transient species must have time to reorient before it can absorb the “perpendicularly” polarized light.

Once the parallel and perpendicular traces have been measured, an anisotropy plot is constructed with the following formula:

$$anisotropy = \frac{I_{para} - I_{perp}}{I_{para} + 2I_{perp}} \quad (1)$$

The numerator of the equation represents the difference between the parallel and perpendicular intensities. The denominator represents the total intensity. When adding the x, y, and z components of the intensity, the parallel intensity represents the z component since the parallel pulse is aligned with the z axis. The perpendicular intensity represents a superposition of the x and y components. Fitting the anisotropy data to an exponential gives the rotational reorganization lifetime of the compound of interest.

Anisotropy can be removed from a system through use of “magic angle” conditions. Under such conditions, both polarizers are set to  $54.7^\circ$  from vertical. As described by Lakowicz, “the use of these conditions results in a signal proportional to the total intensity...”<sup>5</sup>

## 1.5. Transient Absorption

The transient absorption techniques used in this thesis were pump-probe techniques. In such techniques, the sample is first irradiated by the “pump” pulse which excites the molecule of interest to the  $S_1$  state. After a carefully defined delay, the “probe” pulse hits the sample, exciting the molecule from the  $S_1$  state to a higher-energy  $S_n$  state.

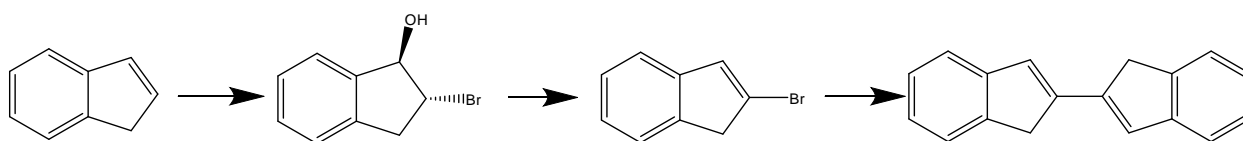
Because the  $S_1$  state generally has a very short lifetime, very short pulses of light must be used to obtain meaningful data. Both the single-wavelength and broadband systems used in this thesis employ femtosecond laser systems to provide pulses of requisite shortness. Instrument response functions for the systems employed were between 150 and 250 fs.<sup>10</sup>

The pump-probe delay was controlled through use of a computer-controlled delay stage. The probe beam is reflected off the mobile mirror whose position is controlled by the data collection program. The delay stage controls the delay by lengthening or shortening the path length of the probe beam while the path length of the pump remains constant.

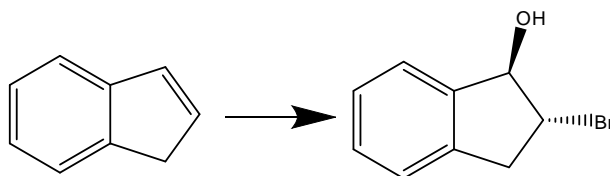
After the delay stage, the probe beam passes through a cuvette of water, resulting in a white light continuum. For single wavelength measurements, a monochromator immediately before the detector selects a wavelength from the continuum. For broadband measurements, a CCD camera acts as the detector, allowing for use of the entire continuum generated.

## 1.6 Synthetic Considerations

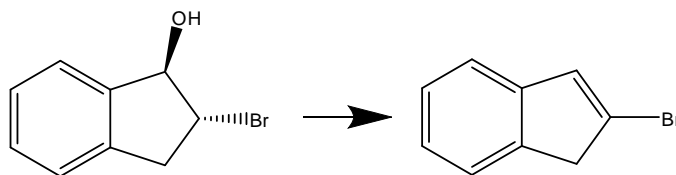
The synthesis of 2,2'-bisindene appears in literature. The synthetic pathway chosen consists of the acid catalyzed dehydration of 2-bromoindanol to yield 2-bromoindene. The 2-bromoindene is then self-coupled to form 2,2'-bisindene. While 2-bromoindanol is commercially available, it was also synthesized in the interest of economy.



The synthesis of 2-bromoindanol was a straightforward reproduction of the literature procedure.<sup>11</sup> The best results were obtained when the n-bromosuccinimide was recrystallized in water to remove n-succinimide, a photodegradation product.

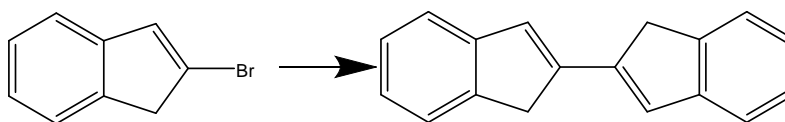


The synthesis of 2-bromoindene was also straightforward; it required few modifications to procedures previously reported.<sup>12, 13</sup> Purification by either chromatography or vacuum distillation proved effective. Distillation was somewhat more impractical since the compound exists as a solid at room temperature and required heating of the distillation glassware.



The synthesis of 2,2'-bisindene was problematic. Repeated attempts following the literature procedure<sup>14</sup> resulted in <1% yields. When methyl iodide was replaced with solid

iodine, the byproducts of the reaction were difficult to characterize, as the brown sludge formed was not soluble in readily available solvents. I hypothesize that the byproducts consist primarily of copper salts and unreacted indene.



## 2. Results and Discussion

### 2.1 Synthesis of 2,2'-Bisindene

#### Experimental Methods

Unless otherwise noted, all reagents and solvents were used as purchased without further purification. Flash chromatography was performed on silica gel with solvent system noted. Nuclear magnetic resonance (NMR) spectra were obtained with a 250 MHz Bruker spectrometer.

**2-Bromoindanol** To a stirring solution of indene (10.93 g, 94 mmol), water (10 mL), and dimethylsulfoxide (100 mL) at 0 °C was added freshly recrystallized n-bromosuccinimide (18.09 g, 102 mmol). After a brief period of time, the resulting yellow suspension became an orange, clear solution. The ice bath was removed and the solution was allowed to warm to room temperature and stir overnight. After ca. 18 h, the orange solution was hydrolyzed at room temperature with 120 mL water. The resulting suspension was extracted with diethyl ether (3 x) and the combined organic extracts were dried and evaporated to afford a yellow amorphous solid. The solid was recrystallized from chloroform/hexane to afford 12.42 g (62%) of 2-bromoindanol as colorless crystals.  $^1\text{H}$  NMR ( $\text{CDCl}_3$ , 250 MHz)  $\delta_{\text{H}}$  7.11-7.35 (m, 4 H, aromatic), 5.20 (d, 1 H), 4.17 (q, 1 H), 3.48 (q, 1 H), 3.12 (q, 1 H), 2.59 (s, 1 H, OH);  $^{13}\text{C}$  NMR ( $\text{CDCl}_3$ , 62.5 MHz)  $\delta_{\text{C}}$  141.6, 139.7, 128.9, 127.6, 124.5, 124.0, 83.3, 54.5, 40.4.

**2-Bromoindene** A suspension of 2-bromoindanol (12.42 g, 58.3 mmol) and pTSA (0.775 g, 4.1 mmol) in benzene was heated to reflux and allowed to stir ca. 3 h. The benzene was then evaporated *in vacuo*. To the resulting oil was added 100 mL diethyl ether. The solution was washed ( $\text{NaHCO}_3$  x 3,  $\text{H}_2\text{O}$  x1) and dried ( $\text{MgSO}_4$ ). Upon vacuum filtration of the drying agent, a white solid, presumably 2-bromoindanol precipitated. TLC (1:1 hexanes-ethyl acetate) of the crude

product revealed the presence of starting material. The crude solid was redissolved in 100 mL toluene and ca. 1 mL concentrated sulfuric acid was added. The solution was heated to reflux for ca. 24 h. After cooling, the toluene was evaporated *in vacuo* and 60 mL diethyl ether was added to the resulting oil. The solution was washed (NaHCO<sub>3</sub> x2, H<sub>2</sub>O x2), dried (MgSO<sub>4</sub>), and evaporated to afford a red-brown oil. The oil was flash chromatographed (hexanes) to afford a colorless oil. Upon standing at room temperature, 2-bromindene (3.87 g, 34%) precipitated as colorless crystals. Mp 36-37 °C; <sup>1</sup>H NMR (CDCl<sub>3</sub>, 250 MHz) δ<sub>H</sub> 7.12-7.37 (m, 4 H), 6.92 (s, 1 H), 3.58 (s, 2 H); <sup>13</sup>C NMR (CDCl<sub>3</sub>, 62.5 MHz) δ<sub>C</sub> 144.0, 142.6, 133.0, 126.7, 124.9, 124.8, 123.2, 120.2, 45.44.

**2,2'-Bisindene** Magnesium turnings (0.738 g, 30.4 mmol) were suspended in 30 mL freshly distilled THF under nitrogen atmosphere and activated with iodine crystals. A solution of 2-bromoindene (5.87 g, 30.2 mmol) in dry THF was dropped slowly into the Mg suspension. The solution changed from colorless to red and began to reflux. The solution was then heated to maintain reflux for 2.5 h. After cooling to 0 °C, freshly flame-dried CuCl<sub>2</sub> (4.073 g, 30.4 mmol) was added to the solution. The resulting suspension was allowed to warm to room temperature and stir for 18 h. The resulting black suspension was filtered and washed (dry THF x3, dry ether x3). Upon washing with ether, a brown solid precipitated from the filtrate. The brown solid was collected and recrystallized from toluene with a Craig tube apparatus to afford 2,2'-bisindene (116 mg, 1.6%) as a light brown powder. <sup>1</sup>H NMR (CDCl<sub>3</sub>, 250 MHz) δ<sub>H</sub> 7.03-7.30 (m, 4 H), 6.62 (s, 1 H), 3.35 (s, 2 H); <sup>13</sup>C NMR (CDCl<sub>3</sub>, 62.5 MHz) δ<sub>C</sub> 145.3, 143.4, 143.0, 127.9, 126.6, 124.9, 123.6, 120.9, 38.7.

## 2.2. Absorption and Fluorescence Spectra

All steady-state spectra were measured in chloroform in quartz sample cells. For the emission spectrum, the excitation monochromator of the fluorimeter was set to 350 nm and the emission wavelength was scanned. For the excitation spectrum, the detector monochromator was set to 410 nm and the excitation wavelength was scanned. The steady state spectra observed were quite similar to those reported for DPB, suggesting that rotational motion of the phenyl groups has little effect on the steady-state spectroscopy of DPB. Figure 2.2.1 shows the normalized steady-state spectra observed.

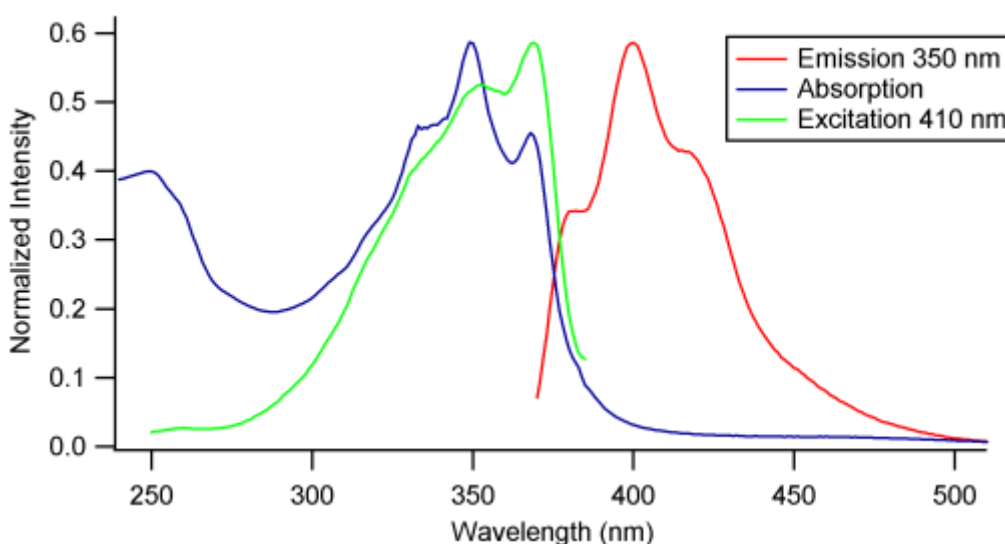


**Figure 2.2.1. Normalized Steady-State Absorption and Fluorescence Spectra**

### 2.3. TCSPC Lifetime and Anisotropy

TCSPC measurements were performed in chloroform with a quartz sample cell. The sample was pumped at 310 nm. Before each measurement, the samples were degassed by bubbling Ar gas through the sample for 10 min. This degassing prevented quenching of fluorescence by oxygen gas in solution. The detection wavelength was varied between 390 and



400 nm as indicated. Magic angle conditions were used for measurement of fluorescence decay lifetimes. For anisotropy measurements, the vertical, “parallel,” angle was found to be 359°, the “perpendicular” angle was found to be 89°. To facilitate data analysis, an arbitrary channel in the “tail” region of the decay was chosen as a tail-matching point. Data collection was stopped when 10,000 counts were collected in the specified channel for the parallel and perpendicular traces to eliminate the need to tail-match the data.

Fluorescence decay lifetimes were calculated with a deconvolution program written by the Gustafson group to deconvolve the instrument response function from the observed data. Biexponential decays were observed. Table 2.3.1 shows the lifetimes obtained. Figure 2.3.1 shows a representative fluorescence decay trace with fitting function included.

**Table 2.3.1. Fluorescence Decay Lifetimes by TCSPC**

Delay (ns)	Detection Wavelength ( $\lambda$ )	$\tau_1$	$\tau_2$
25	400	$1.052 \pm 0.005$	$0.134 \pm 0.003$
25	390	$1.001 \pm 0.005$	$0.116 \pm 0.003$
10	400	$1.025 \pm 0.003$	$0.113 \pm 0.002$

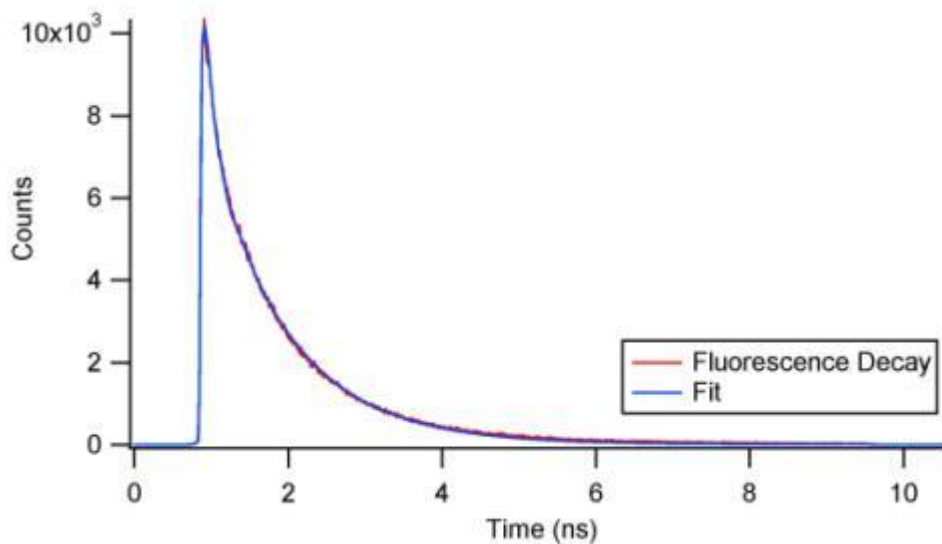


**Figure 2.3.1: Fluorescence Decay – 10 ns Delay, 400 nm Detection**

The anisotropy curve was calculated according to equation 1.4.1 with no additional tail fitting. The instrument delay was set to 2.5 ns and the detector monochromator was set to 400 nm for the anisotropy measurements. An exponential was fitted to give a rotational reorganization lifetime of  $75.8 \pm 0.7$  ps. Figure 2.3.2 shows the parallel and perpendicular decays; figure 2.3.3 shows the calculated anisotropy curve and exponential fitting function.

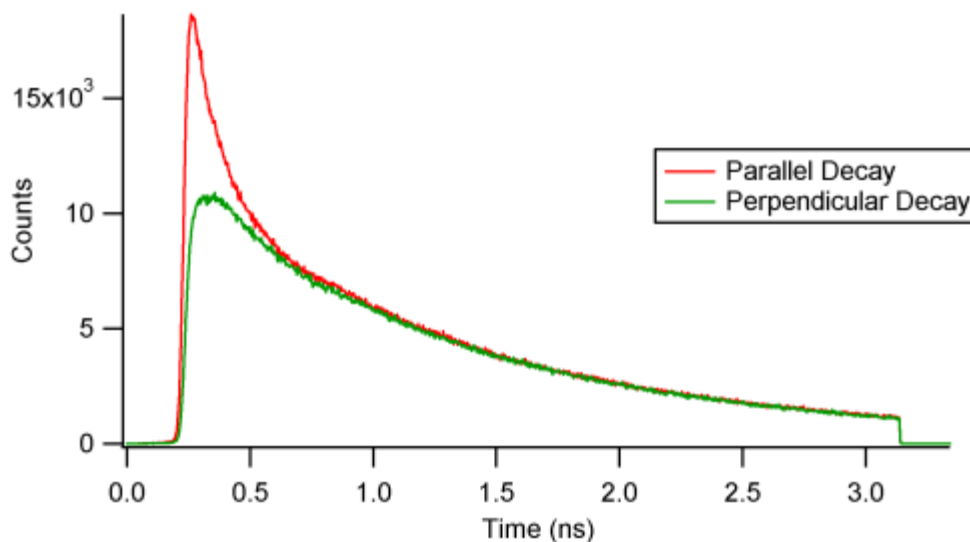


**Figure 2.3.2. Parallel and Perpendicular Decay**

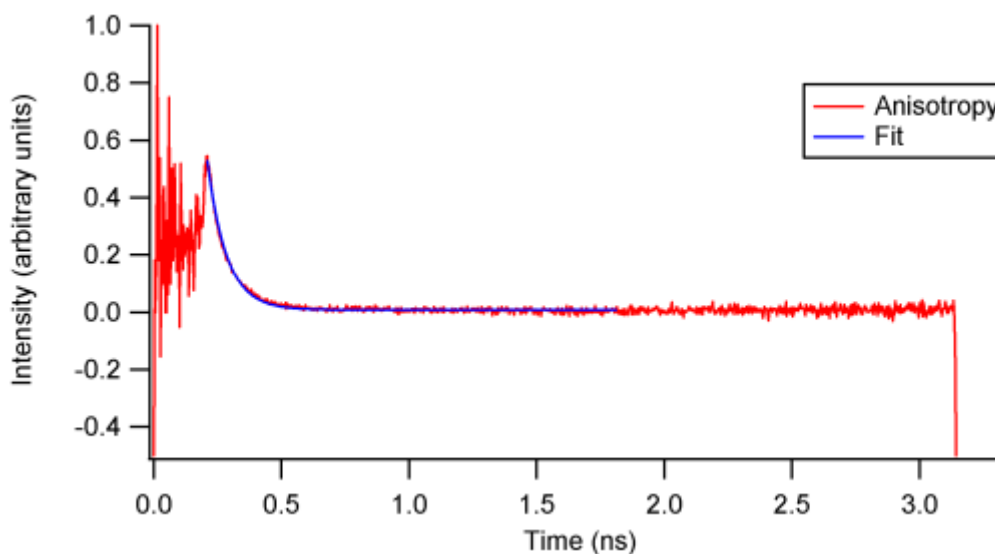


**Figure 2.3.3. Anisotropy Curve and Fitted Exponential**

#### **2.4. Pump-Probe Transient Absorption Anisotropy**

Pump-probe kinetic traces were performed with chloroform as the solvent. The sample was measured in a flow cell to prevent photodegradation. The pump wavelength was 372 nm and the probe wavelength was 600 nm. The vertical, parallel, polarization angle was found to be  $127^\circ$  and the perpendicular polarization angle was  $217^\circ$ . Five traces were gathered and averaged

for both the perpendicular and parallel traces. After each set of five traces, the initial intensity,  $I_0$  was recorded to allow for calculation of  $\Delta O.D.$  values as outlined by Hare.<sup>10</sup> Once the intensity values had been converted to  $\Delta O.D.$  values, the parallel and perpendicular decays were tail-matched and the anisotropy was calculated according to equation 1.4.1. An exponential function was fitted to the anisotropy decay. The rotational reorganization lifetime was found to be  $29.7 \pm 1.4$  ps. Figure 2.4.1 shows the parallel and perpendicular decay traces; figure 2.4.2 shows the anisotropy decay and fitted exponential function.

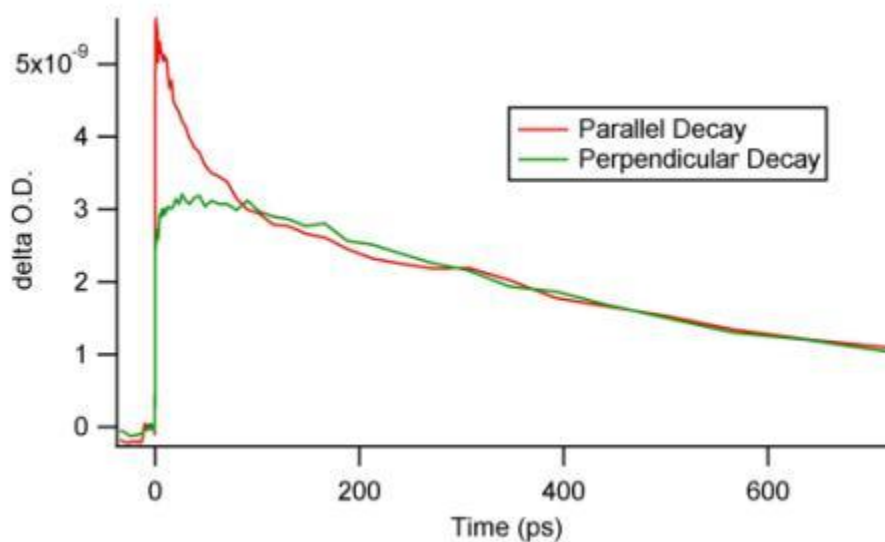


**Figure 2.4.1. Parallel and Perpendicular Decay Traces Measured by Transient Absorption**

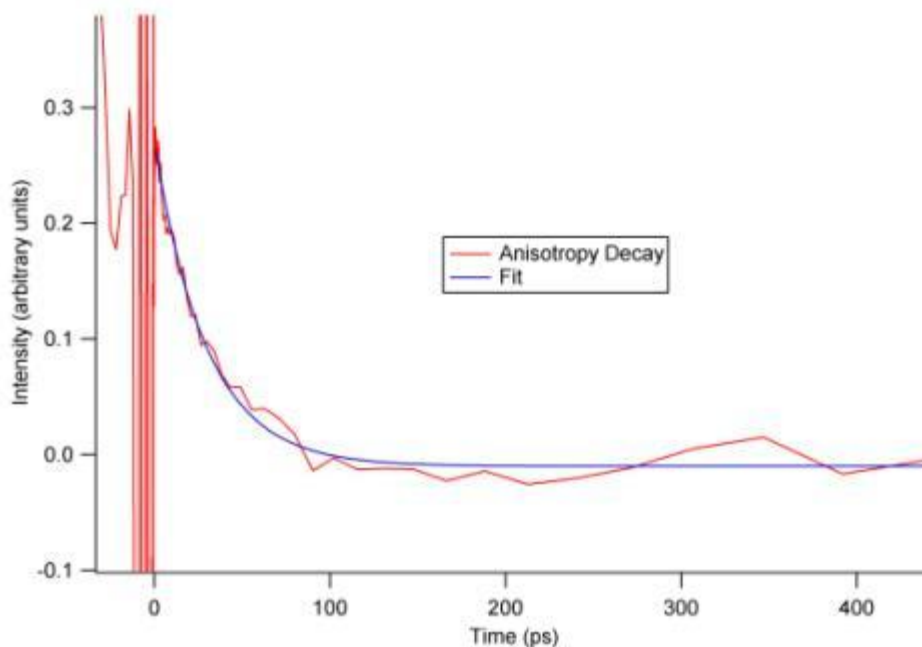


**Figure 2.4.2. Anisotropy Decay and Exponential Fit Measured by Transient Absorption**

## **2.5. Broadband Transient Absorption**

Broadband transient absorption measurements were performed with solutions in chloroform. While chloroform is not an optimal solvent for ultrafast studies, 2,2'-bisindene was found to be insoluble in other practical solvents. The sample was analyzed in a flow cell to prevent photodegradation. The sample was pumped at 337 nm. The CCD detector was calibrated such that data was collected between roughly 370 nm and 710 nm. Data collected at wavelengths shorter than 475 nm were disregarded due to the strong fluorescence bleaching of the sample. The data from two consecutive runs was averaged and the baseline spectrum taken at a -1 ps delay was subtracted from the spectra.

Two transient absorption bands are observed: one at 545 nm and one at 625 nm. The band at 545 nm exhibits some peak shifting over the course of the experiment. The kinetic traces

at both wavelengths show an unusually long (50 ps) rise time. These two spectral features are most likely due to conformational relaxation in solution.

Exponential functions were fitted to kinetic traces measured at both peak wavelengths. The lifetime of the 545 nm trace was  $580 \pm 30$  ps. The lifetime of the 625 nm trace was  $630 \pm 30$  ps. Within error, the lifetimes obtained appear to be identical. These lifetimes are shorter than the lifetime obtained with TCSPC. This is likely because the transient absorption samples were not argon purged and were thusly subject to oxygen quenching. Figures 2.5.1 and 2.5.2 show the kinetic traces observed and the exponential fitting functions used.

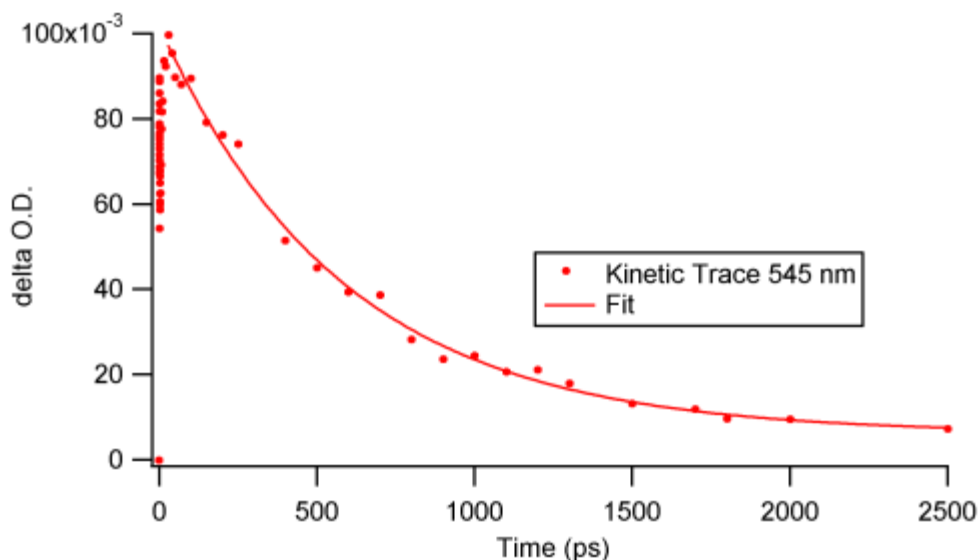


**Figure 2.5.1. Kinetic Trace at 545 nm**

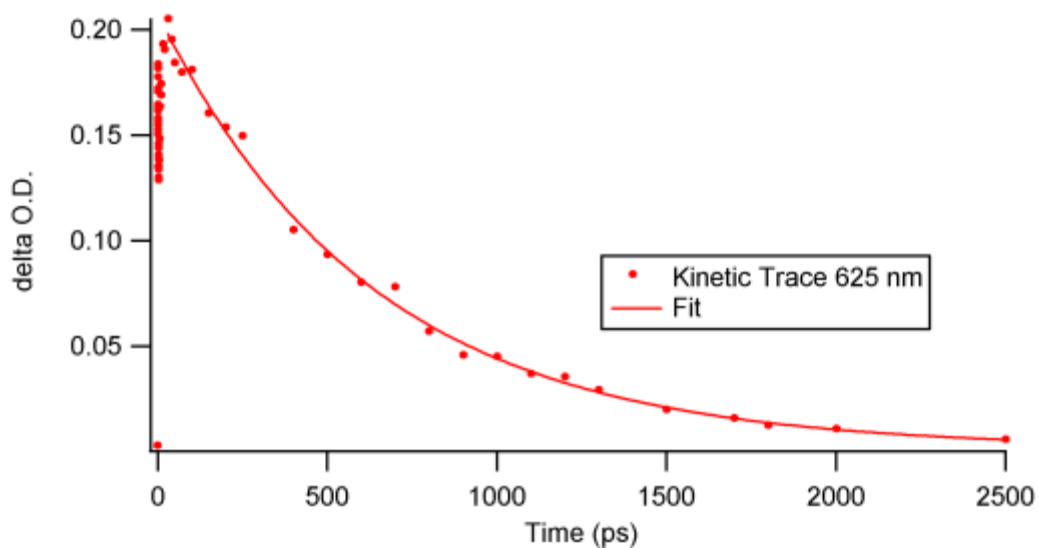


**Figure 2.5.2. Kinetic Trace at 625 nm**

Due to the unusually long rise time, the absorption traces exhibit unusual ordering before 50 ps. Figure 2.5.3 shows selected traces. The shifting of the 545 nm band and the atypical ordering are evident.

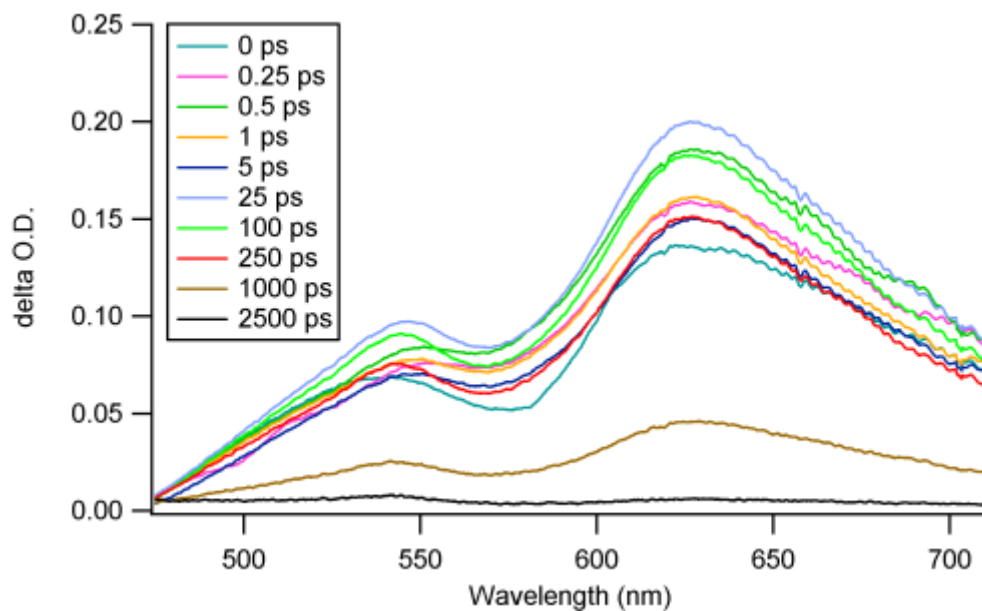


**Figure 2.5.3. Selected Transient Absorption Traces**

### 3. Conclusion and Future Directions

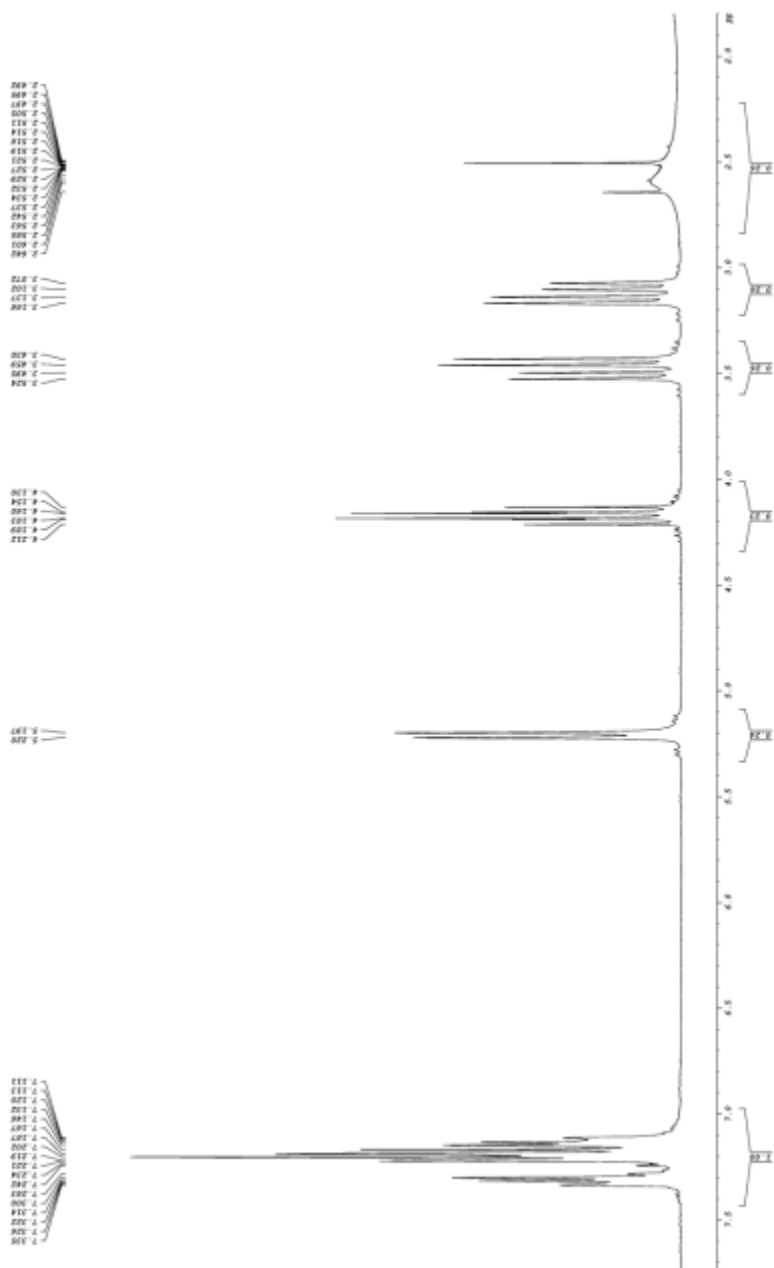
From the steady-state spectra and the fluorescence lifetimes it appears that the rotational motion of the phenyl groups has little effect on the excited state dynamics of DPB. The transient absorption data show what appears to be strong influence from conformational relaxation. This coincides with the expectation that the conformation of DPB about the central single bond gives rise to DPB's unusual excited state dynamics.

The rotational reorganization lifetimes offer a more puzzling result. It is expected that the lifetimes obtained from TCSPC and transient absorption methods should be equivalent. This is not the case for the data collected. This problem must be studied further. The two measurements must be repeated and the parameters of the experiment (pump wavelength, probe/detection wavelength, etc...) must be varied to determine whether the reorganization lifetimes are actually different or if these data represent an experimental anomaly.

Time-resolved vibrational spectroscopy of 2,2'-bisindene should also be explored. It stands to reason that the constriction of rotation would more strongly affect the vibrational spectra than the electronic spectra. The rotational structure of 2,2'-bisindene is obviously much different from that of DPB. Through constraint of the rotation of the phenyl bonds, it should be possible to more closely study the vibrational behavior of the central single bond of DPB.



### NMR Spectra of Synthesized Compounds (CDCl<sub>3</sub>)



29

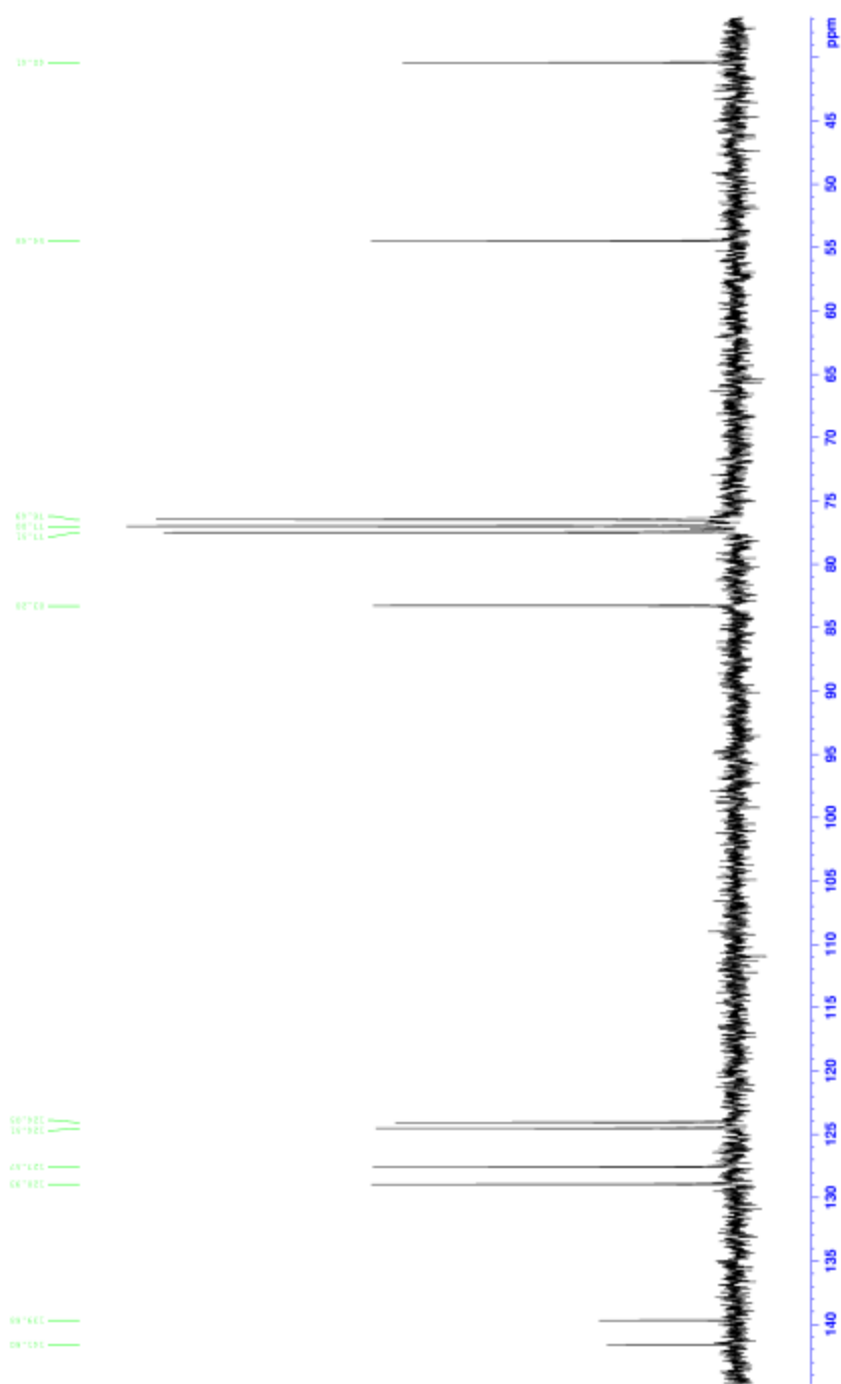


Figure A.2.  $^{13}\text{C}$  Spectrum of 2-Bromoindanol

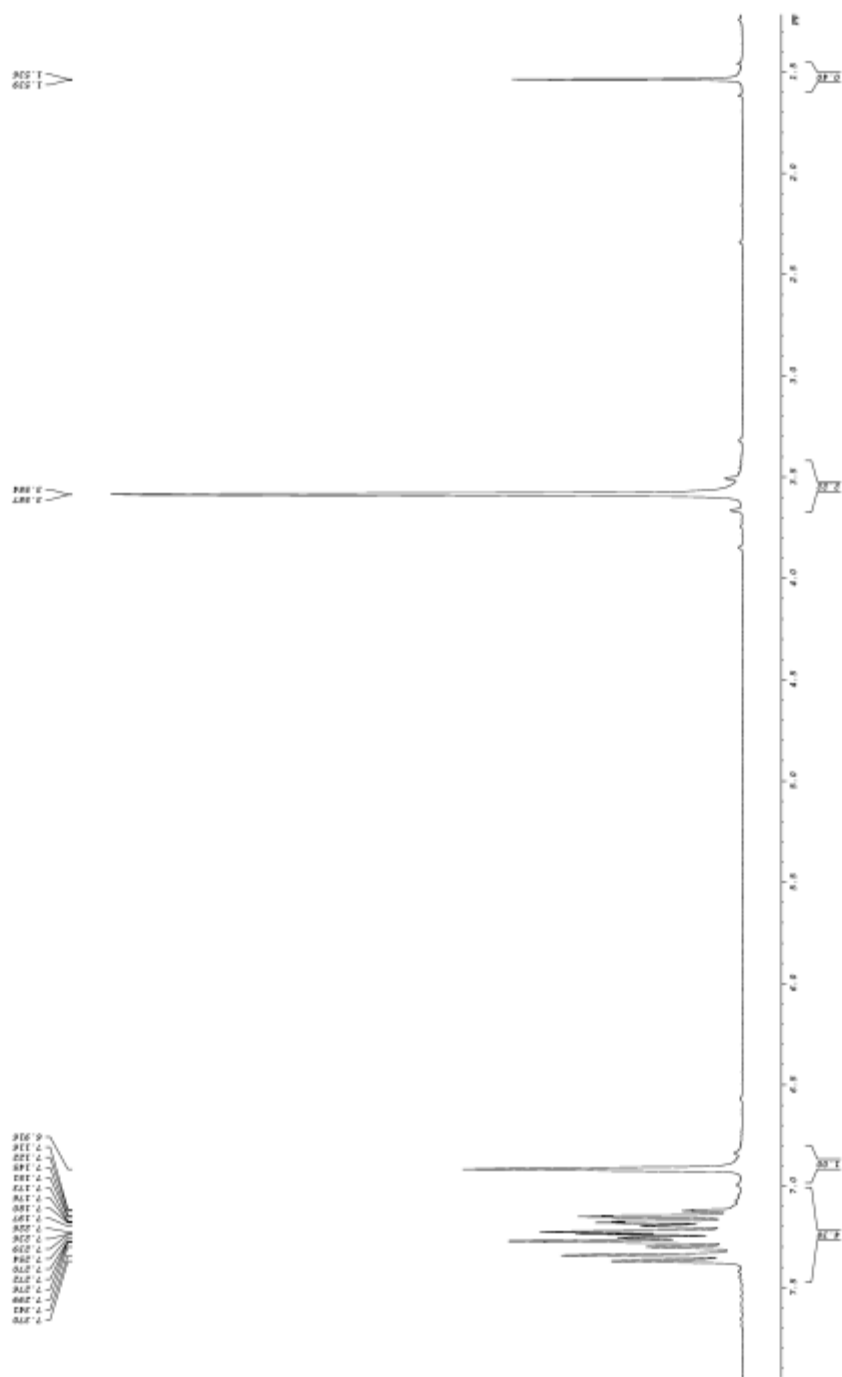
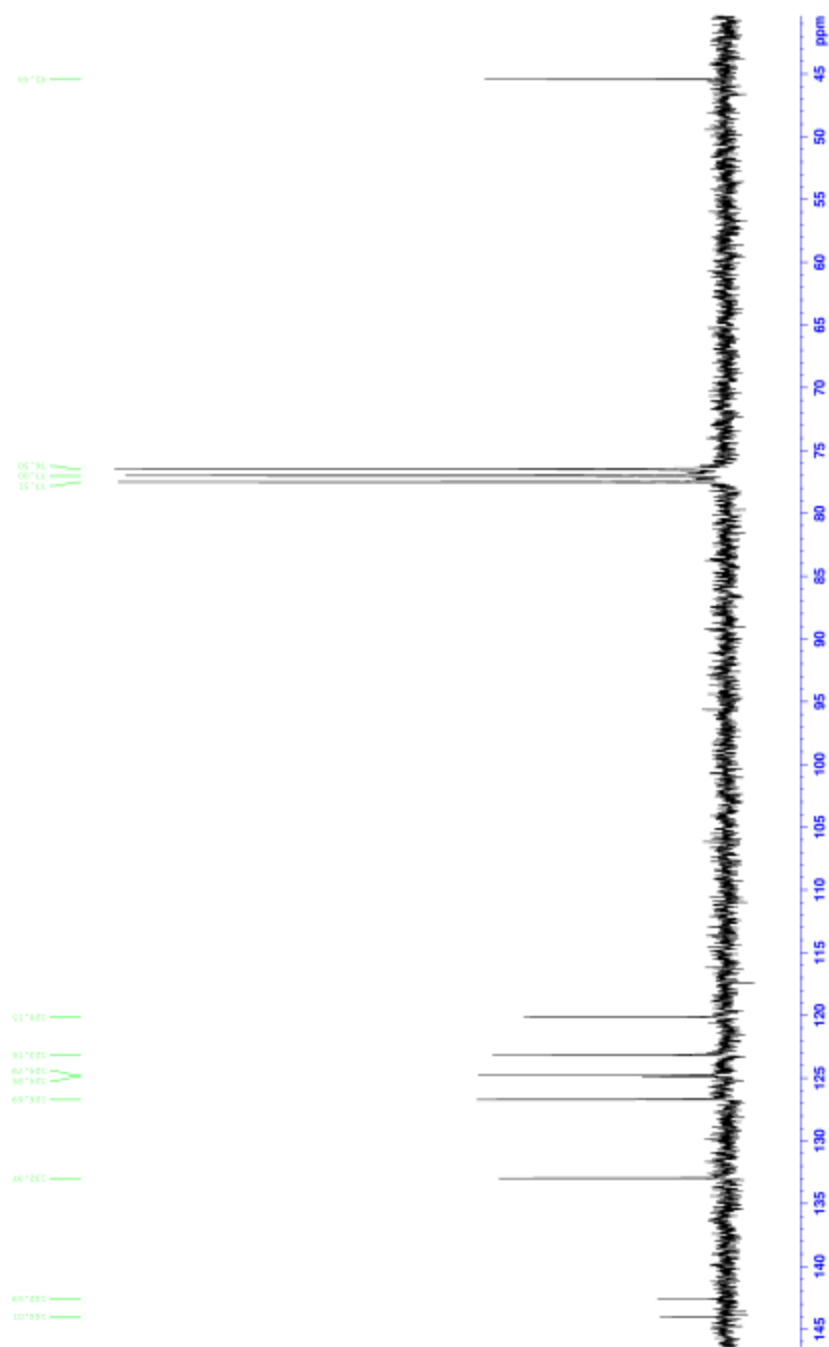


Figure A.3.  $^1\text{H}$  Spectrum of 2-Bromoindene



**Figure A.4.**  $^{13}\text{C}$  Spectrum of 2-Bromoindene

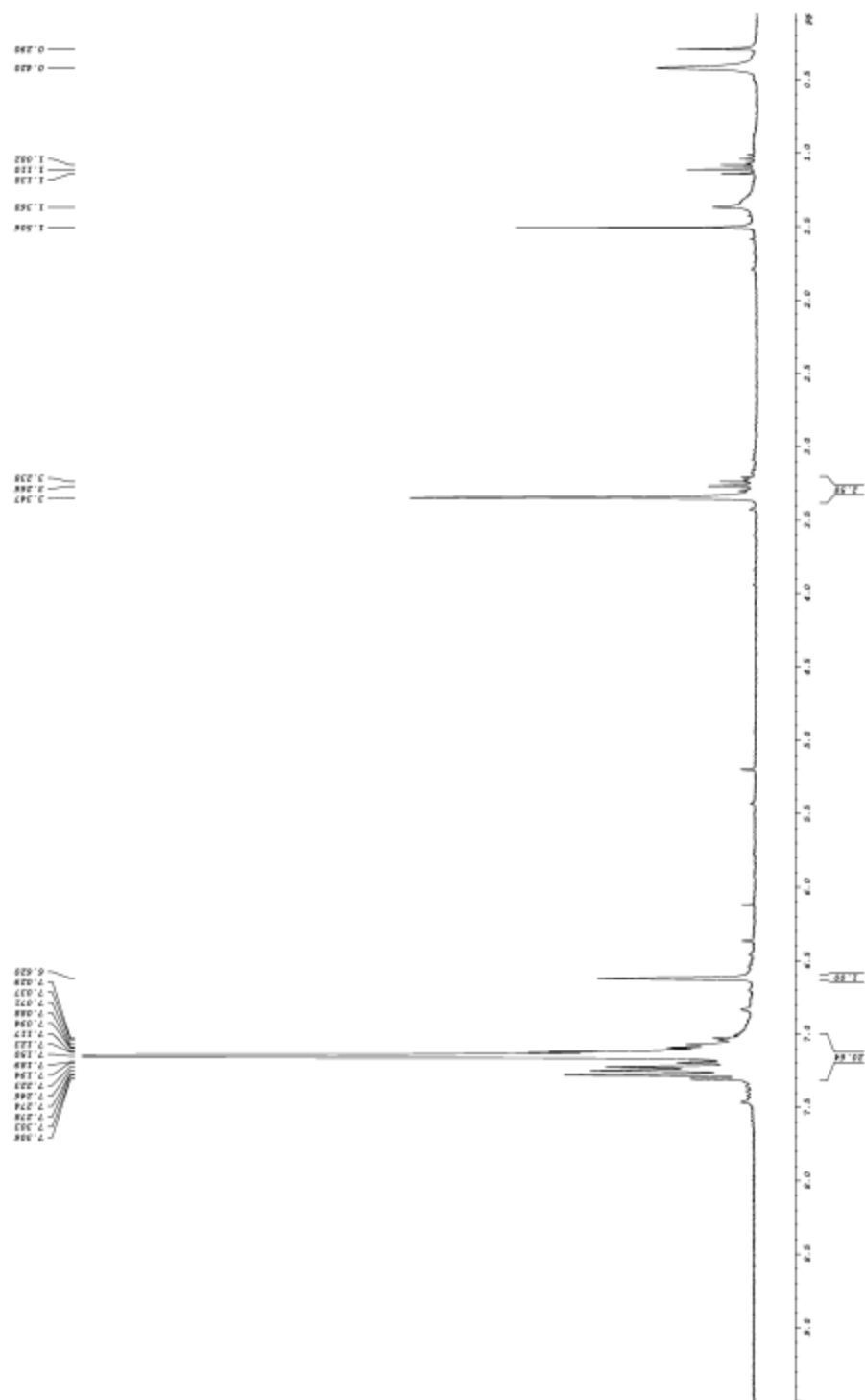


Figure A.4.  $^1\text{H}$  Spectrum of 2,2'-Bisindene (Solvent Peaks Not Integrated)

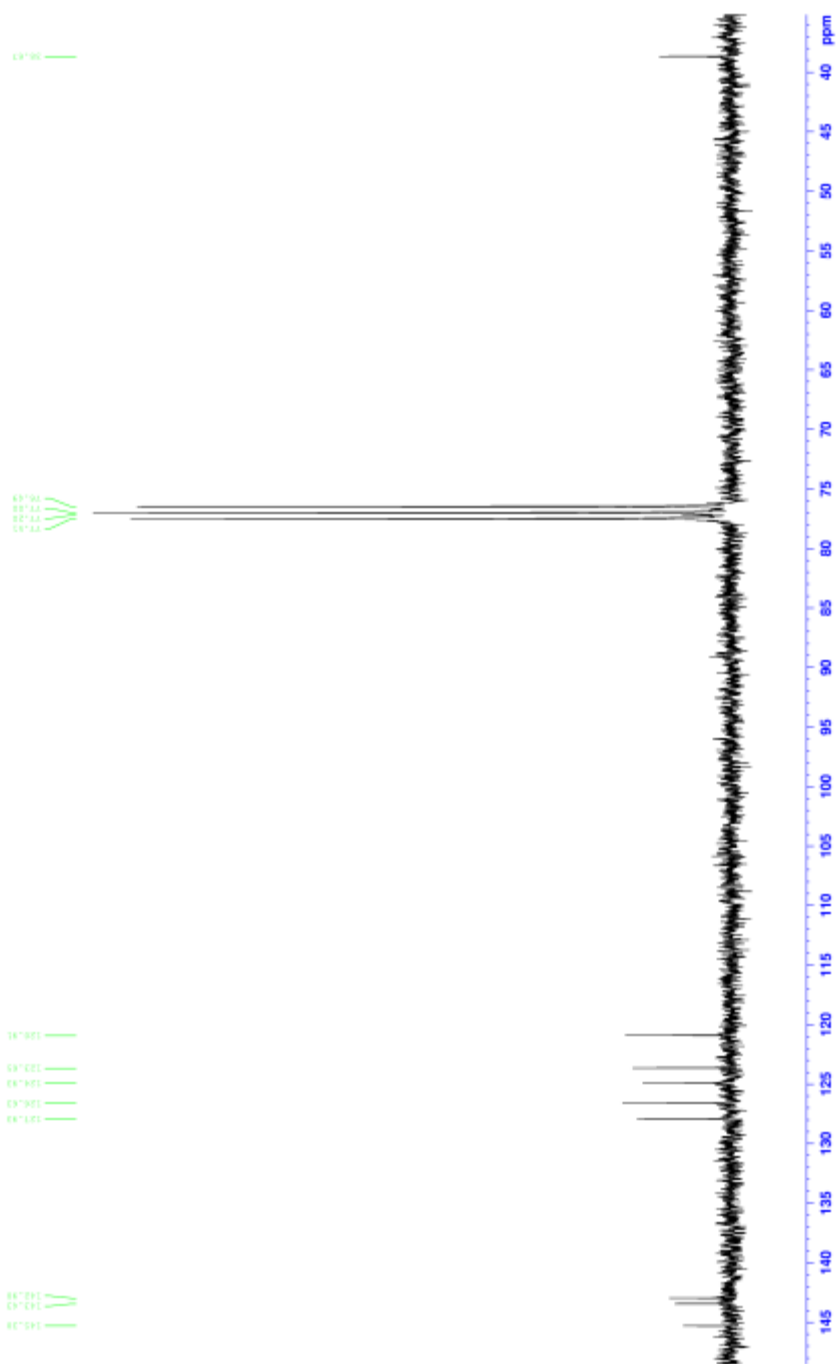


Figure A.6. <sup>13</sup>C Spectrum of 2,2'-Bisindene

## References

- 1.) Brown, P. K.; Wald, G. *J. Biol. Chem.* **1956**, *222*, 865-877
- 2.) "Medicine 1967," [www.nobelprize.org](http://www.nobelprize.org) (accessed 10 April, 2007)
- 3.) Yee, W. A.; Horwitz, J. S.; Goldbeck, R. A.; Elnterz, C. M.; Kilger, D. S. *J. Phys. Chem.* **1983**, *87*, 380-382
- 4.) O'Connor, D. V.; Phillips, D. Time-correlated Single Photon Counting; Academic Press: London, 1984
- 5.) Lakowicz, J.R. Principles of Fluorescence Spectroscopy; Springer: New York, NY, 2004
- 6.) Canonica, S.; Kramer, J. B.; Reiss, D.; Gygax, H. *Environ. Sci. Technol.* **1996**, *31*, 1754-1760
- 7.) Petrov, N. Kh.; Gulakov, M. N.; Alfimov, M. V.; Busse, G.; Frederichs, B.; Techert, S. *J. Phys. Chem. A* **2003**, *107*, 6341-6344
- 8.) Seixas de Melo, J.; Rondao, R.; Burrows, H. D.; Melo, M. J.; Navaratnam, S.; Edge, R.; Voss, G. *J. Phys. Chem. A* **2006**, *110*, 13653-13661
- 9.) Karatsu, T.; Itoh, H.; Nishigaki, A.; Fukui, K.; Kitamura, A.; Matsuo, S.; Misawa, H. *J. Phys. Chem. A* **2000**, *104*, 6993-7001
- 10.) Hare, P. M. PhD. thesis, The Ohio State University, Columbus, OH, 2007
- 11.) Lindley, W. A.; McDowell, D. W. H. *J. Org. Chem.* **1982**, *47*, 705-709
- 12.) McEwen, I.; Roennqvist, M.; Ahlberg, P. *J. Am. Chem. Soc.* **1993**, *115*, 3989-3996
- 13.) Halterman, R. L.; Fahey, D. R.; Bailly, E. F.; Dockter, D. W.; Stenzel, O.; Shipman, J. L.; Khan, M. A.; Dechert, S.; Schumann, S. *Organometallics* **2000**, *19*, 5464-5470
- 14.) Tews, D.; Gaede, P. E. *Organometallics* **2001**, *20*, 3869-3875